JCB Article

L1-dependent neuritogenesis involves ankyrin$_B$ that mediates L1-CAM coupling with retrograde actin flow

Kazunari Nishimura,[1] Fumie Yoshihara,[1] Takuro Tojima,[1,2] Noriko Ooashi,[1] Woohyun Yoon,[3] Katsuhiko Mikoshiba,[2] Vann Bennett,[3] and Hiroyuki Kamiguchi[1]

[1]Laboratory for Neuronal Growth Mechanisms, Brain Science Institute, Institute of Physical and Chemical Research (RIKEN), Saitama 351-0198, Japan
[2]Division of Molecular Neurobiology, The Institute of Medical Science, The University of Tokyo, Tokyo 108-8639, Japan
[3]Howard Hughes Medical Institute and Departments of Cell Biology and Biochemistry, Duke University Medical Center, Durham, NC 27710

The cell adhesion molecule L1 (L1-CAM) plays critical roles in neurite growth. Its cytoplasmic domain (L1CD) binds to ankyrins that associate with the spectrin–actin network. This paper demonstrates that L1-CAM interactions with ankyrin$_B$ (but not with ankyrin$_G$) are involved in the initial formation of neurites. In the membranous protrusions surrounding the soma before neuritogenesis, filamentous actin (F-actin) and ankyrin$_B$ continuously move toward the soma (retrograde flow). Bead-tracking experiments show that ankyrin$_B$ mediates L1-CAM coupling with retrograde F-actin flow in these perisomatic structures. Ligation of the L1-CAM ectodomain by an immobile substrate induces L1CD–ankyrin$_B$ binding and the formation of stationary ankyrin$_B$ clusters. Neurite initiation preferentially occurs at the site of these clusters. In contrast, ankyrin$_B$ is involved neither in L1-CAM coupling with F-actin flow in growth cones nor in L1-based neurite elongation. Our results indicate that ankyrin$_B$ promotes neurite initiation by acting as a component of the clutch module that transmits traction force generated by F-actin flow to the extracellular substrate via L1-CAM.

Introduction

Complex neural networks are formed by nerve processes that have emerged and elongated from nascent neurons. Various functional molecules, including cell adhesion molecules (CAMs) and cytoskeletal elements, are cooperatively involved in process outgrowth. Developmental defects in major axon tracts, such as the corpus callosum and the corticospinal tract, are found in humans with X-linked hydrocephalus that is caused by mutations in the gene of cell adhesion molecule L1 (L1-CAM), a member of the Ig superfamily of CAMs (Kamiguchi et al., 1998). L1-CAM is a single-pass transmembrane protein that is predominantly expressed by developing neurons, and promotes neuronal migration and neurite growth. Human pathogenic mutations in the L1-CAM cytoplasmic domain (L1CD) produce less severe phenotypes than those in the L1-CAM extracellular domain (L1ED). However, mutations in the L1CD almost always cause abnormal axon tract development, suggesting that the L1CD is critical for axon growth (Kamiguchi et al., 1998). The majority of mutations in the L1CD reported so far are either nonsense or frame shift mutations that produce a premature stop codon (Van Camp et al., 1996), eliminating its COOH-terminal tail that contains a binding site for ankyrins. The amino acid residues SFIGQY^{1229} in the human L1CD are conserved among the majority of L1 family CAMs including NrCAM and neurofascin (Hortsch, 2000), and are critical for their ankyrin-binding activity (Garver et al., 1997; Hortsch et al., 1998a).

The ankyrin family currently includes three genes encoding for ankyrin$_R$, ankyrin$_G$, and ankyrin$_B$, as well as multiple alternatively spliced variants (Bennett and Chen, 2001). 480/270-kD ankyrin$_G$ and 440/220-kD ankyrin$_B$ are the major isoforms expressed in the developing nervous system. Ankyrins interact with structurally diverse membrane proteins,

The online version of this article includes supplemental material.

Address correspondence to Hiroyuki Kamiguchi, Laboratory for Neuronal Growth Mechanisms, RIKEN Brain Science Institute, 2-1 Hirosawa, Wako, Saitama 351-0198, Japan. Tel.: 81-48-467-6137. Fax: 81-48-467-9795. email: kamiguchi@brain.riken.jp

Key words: ankyrin; L1-CAM; adhesion; neurite; clutch

Abbreviations used in this paper: CAM, cell adhesion molecule; DIC, differential interference contrast; DRG, dorsal root ganglion; FRET, fluorescent resonance energy transfer; FRET^E, FRET efficiency; L1-CAM, cell adhesion molecule L1; L1CD, L1-CAM cytoplasmic domain; L1ED, L1-CAM extracellular domain.

including ion channels and L1 family CAMs, through ANK repeats in their membrane-binding domains. Ankyrins also associate with the spectrin–actin network via their spectrin-binding domains, thereby coupling the membrane proteins to the actin cytoskeleton. L1-CAM and ankyrin$_B$ are colocalized in premyelinated axon tracts during development. Ankyrin$_B^{(-/-)}$ mice exhibit axon tract hypoplasia similarly to L1-CAM$^{(-/Y)}$ mice and X-linked hydrocephalus patients (Scotland et al., 1998). Furthermore, missense point mutations in the ankyrin-binding region of the L1CD, Y1229H and S1224L, are sufficient to produce the phenotype in humans (Van Camp et al., 1996), suggesting that the interaction of L1-CAM with ankyrins plays an important role in axon growth. However, it remains to be determined whether and how ankyrins are involved in axon growth stimulated via L1-CAM.

Generally, it is thought that cell migration and process outgrowth are driven by traction force generated by F-actin that flows in a backward direction (Lin and Forscher, 1995; Mitchison and Cramer, 1996). CAMs transmit this force by linking the retrograde F-actin flow with immobile ligands present on neighboring cells or in the ECM (Sheetz et al., 1998). For example, several Ig superfamily CAMs, such as apCAM, NrCAM, and L1-CAM, have been shown to couple with retrograde F-actin flow in nerve growth cones (Suter et al., 1998; Faivre-Sarrailh et al., 1999; Kamiguchi and Yoshihara, 2001), thereby promoting neurite elongation. It has also been hypothesized that the initial formation of neurites is induced by coupling between extracellular substrates and retrograde F-actin flow in membranous protrusions surrounding the soma (Smith, 1994). However, poorly understood is the molecular identity of the clutch module that mediates CAM–actin linkages during neurite formation and elongation. The present work shows that L1-dependent neuritogenesis involves an interaction between ankyrin$_B$ and the SFIGQY-containing region in the L1CD, and that this interaction mediates L1-CAM coupling with retrograde F-actin flow. We propose that ankyrin$_B$ constitutes the clutch module that regulates neurite initiation stimulated by L1 family CAMs.

Results

L1CD–ankyrin$_B$ interactions are induced by L1ED ligation

The interaction of ankyrins (270-kD ankyrin$_G$ and 220-kD ankyrin$_B$) with the L1CD was tested indirectly by the ankyrin recruitment assay as described previously (Zhang et al., 1998). When HEK 293 cells were transfected with an expression plasmid coding for either GFP-tagged ankyrin$_G$ (Zhang et al., 1998) or GFP-tagged ankyrin$_B$ (Mohler et al., 2002), the fluorescent signals were diffusely distributed in the cytoplasm with slight enrichment along the plasma membrane (Fig. 1, A and B). This indicates that endogenous spectrin and other ankyrin-binding proteins such as Na/K ATPase in 293 cells were insufficient to recruit the majority of exogenous ankyrins to the plasma membrane. Cotransfection of a neuronal form of L1-CAM caused GFP-ankyrin$_G$ (but not GFP-ankyrin$_B$) to become recruited to the plasma membrane (Fig. 1, C and D). In contrast, cotransfection of

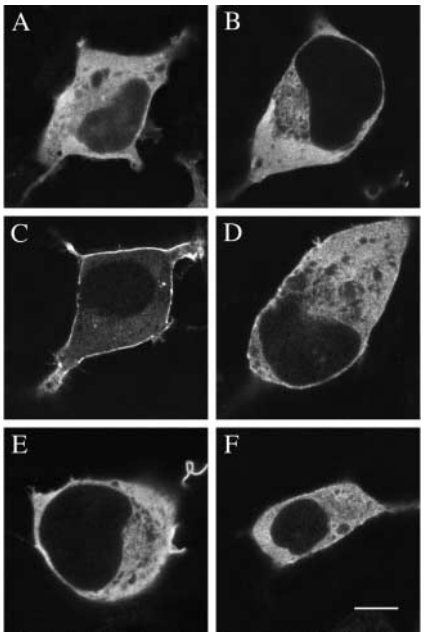

Figure 1. **The L1CD is sufficient for recruitment of exogenous ankyrin$_G$, but not ankyrin$_B$, to the plasma membrane.** Confocal fluorescent images of GFP-ankyrin$_G$ (A, C, and E) and GFP-ankyrin$_B$ (B, D, and F) expressed by 293 cells. The cells did not express L1-CAM (A and B) or did coexpress either wild-type L1-CAM (C and D) or L1-CAM$_{\Delta C77}$ (E and F). L1-CAM expression was visualized by immunofluorescence (not depicted). Bar, 10 μm.

L1-CAM$_{\Delta C77}$, a COOH-terminal truncation mutant that completely lacks the ankyrin-binding region (Kamiguchi and Lemmon, 1998), did not influence the cytoplasmic distribution of GFP-ankyrin$_G$ (Fig. 1 E). These results are consistent with a previous report (Needham et al., 2001) stating that the L1CD expression is necessary and sufficient for recruitment of exogenous ankyrin$_G$ to the plasma membrane. However, our results indicate that the L1CD is not sufficient to recruit ankyrin$_B$ to the plasma membrane.

Next, we examined the distribution pattern of ankyrin$_B$ in contacting cells, because the recruitment of *Drosophila* ankyrin to the plasma membrane was dependent on L1-mediated cell–cell adhesion (Hortsch et al., 1998b). While ankyrin$_B$ remained cytoplasmic in L1-CAM–negative cells in contact (Fig. 2, A and B), L1-CAM coexpression recruited ankyrin$_B$ to the plasma membrane that attaches to the membrane of neighboring L1-CAM–positive cells, but not of L1-CAM–negative cells (Fig. 2, C–E). As controls, human pathogenic mutations in the L1CD, such as ΔC77, Y1229H, and S1224L, impaired L1-CAM's ability to recruit ankyrin$_B$ to cell contact sites (Fig. 2, F–K). These results support the idea that homophilic trans-adhesion via L1-CAM induces ankyrin$_B$ binding to the SFIGQY^{1229}-containing region in the L1CD. Although the L1CD expression was sufficient to recruit ankyrin$_G$ to the plasma membrane (Fig. 1), L1-mediated cell–cell adhesion induced an even greater recruitment of ankyrin$_G$ to the contacting membrane (Fig. 2, L–O).

To further investigate L1-CAM interactions with ankyrin$_B$, we used fluorescent resonance energy transfer (FRET) microscopy using CFP tagged to the COOH terminus of

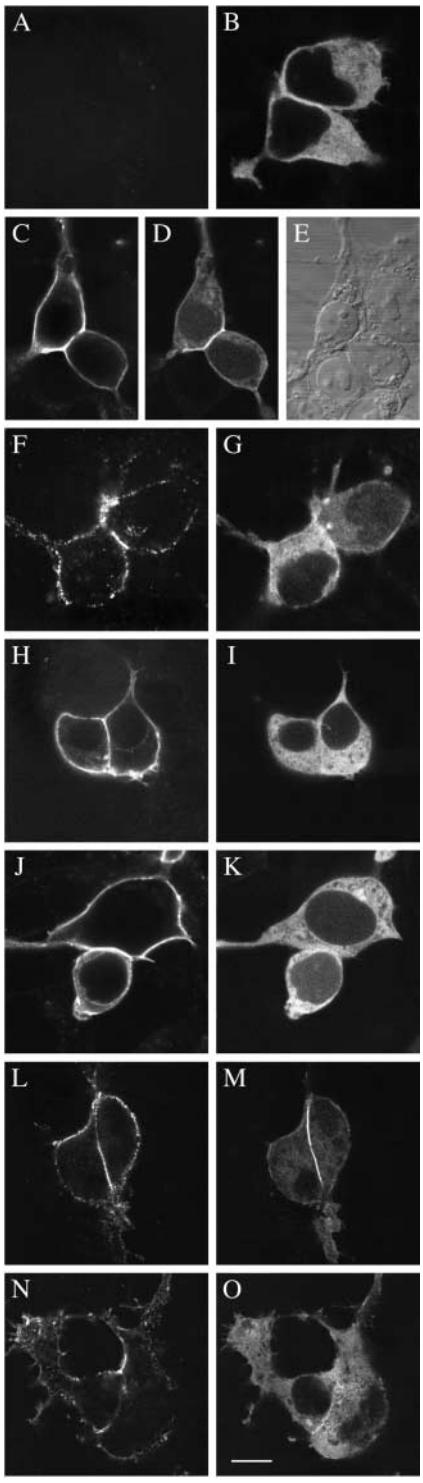

Figure 2. **L1-mediated cell–cell contacts recruit ankyrins to the plasma membrane, which is dependent on the SFIGQY^{1229}-containing region in the L1CD.** (A–K) Confocal images of 293 cells cotransfected with GFP-ankyrin$_B$ and several forms of L1-CAM. Transfected L1-CAM was visualized by immunofluorescence (A, C, F, H, and J), and transfected ankyrin$_B$ by GFP imaging (B, D, G, I, and K). The cells were transfected with the following forms of L1-CAM: wild-type L1-CAM (C–E), L1-CAM$_{\Delta C77}$ (F and G), L1-CAM$_{Y1229H}$ (H and I), or L1-CAM$_{S1224L}$ (J and K). The cells transfected only with GFP-ankyrin$_B$ are also shown (A and B). A DIC image (E) showed the presence of untransfected cells in contact with L1-CAM and ankyrin$_B$-positive cells. (L–O) 293 cells cotransfected with GFP-ankyrin$_G$ and L1-CAM: wild-type L1-CAM (L and M) or L1-CAM$_{\Delta C77}$ (N and O). Transfected L1-CAM was visualized by immunofluorescence (L and N), and transfected ankyrin$_G$ by GFP imaging (M and O). Bar, 10 μm.

the L1CD (L1-CFP) as a donor and Venus tagged to the NH_2 terminus of ankyrin$_B$ (Venus-ankyrin$_B$) as an acceptor. Venus is a variant of YFP with efficient maturation and increased resistance to environmental changes (Nagai et al., 2002). Because FRET from CFP to YFP occurs only if the two proteins are in very close proximity (<50Å), L1-CAM–ankyrin$_B$ interactions should be assessed by measuring FRET efficiency (FRET^E) that is defined as the percentage of donor signal loss due to FRET (Miyawaki and Tsien, 2000). FRET^E can be mathematically deduced from three fluorescent measurements (a donor excitation/donor emission image; a donor excitation/acceptor emission image; and an acceptor excitation/acceptor emission image) after correcting uncertain stoichiometries of CFP to YFP expression and their spectral cross talk (Gordon et al., 1998). Using their method (see Materials and methods), we calculated FRET^E from L1-CFP to Venus-ankyrin$_B$. In 293 cells expressing L1-CFP and Venus-ankyrin$_B$, increased FRET^E was detected at cell contact sites (Fig. 3, A and D). This distribution pattern of increased FRET^E was confirmed by independent measurement using the acceptor photobleaching method (Miyawaki and Tsien, 2000; Fig. 3, I–K). As controls, such an increase in FRET^E at cell contact sites was not observed when a single amino acid mutation, Y1229H (Fig. 3, B and E) or S1224L (Fig. 3, C and F), was introduced to the ankyrin-binding region of L1-CFP. Furthermore, the cross-linking of L1-CAM on the cell surface by anti-L1-CAM antibody increased FRET^E from wild-type L1-CFP to Venus-ankyrin$_B$ in a punctate pattern (Fig. 3 G), whereas the treatment with control antibody had no effect (Fig. 3 H). These results indicate that L1CD–ankyrin$_B$ binding, as assessed by FRET^E, is induced by L1ED ligation.

L1CD–ankyrin$_B$ interactions are involved in L1-stimulated neurite initiation

We tested whether ankyrins are required for neurite growth on an L1-Fc substrate and two other substrates, N-cadherin–Fc and laminin, using ankyrin$_B^{(-/-)}$ and ankyrin$_G^{(-/-)}$ mouse strains described previously (Scotland et al., 1998; Zhou et al., 1998). It has been reported that L1-CAM and N-cadherin presented as a culture substrate stimulate neurite growth in vitro by binding homophilically to L1-CAM and N-cadherin expressed on the neuronal surface, respectively (Lemmon et al., 1989; Bixby and Zhang, 1990). Although heterophilic trans-interactions of L1-CAM with integrins have also been reported (Yip et al., 1998), L1-CAM knockout neurons completely lose their ability to extend neurites on an L1 substrate (Dahme et al., 1997; Fransen et al., 1998), indicating that L1-stimulated neurite growth from mouse neurons depends, for the most part, on homophilic L1-CAM interactions. In contrast, laminin promotes neurite growth upon binding to integrins (Bozyczko and Horwitz, 1986; Tomaselli et al., 1986). As shown in Fig. 4, ankyrin$_B^{(-/-)}$ neurons derived from both the cerebellum and dorsal root ganglion (DRG) had an impaired ability to ini-

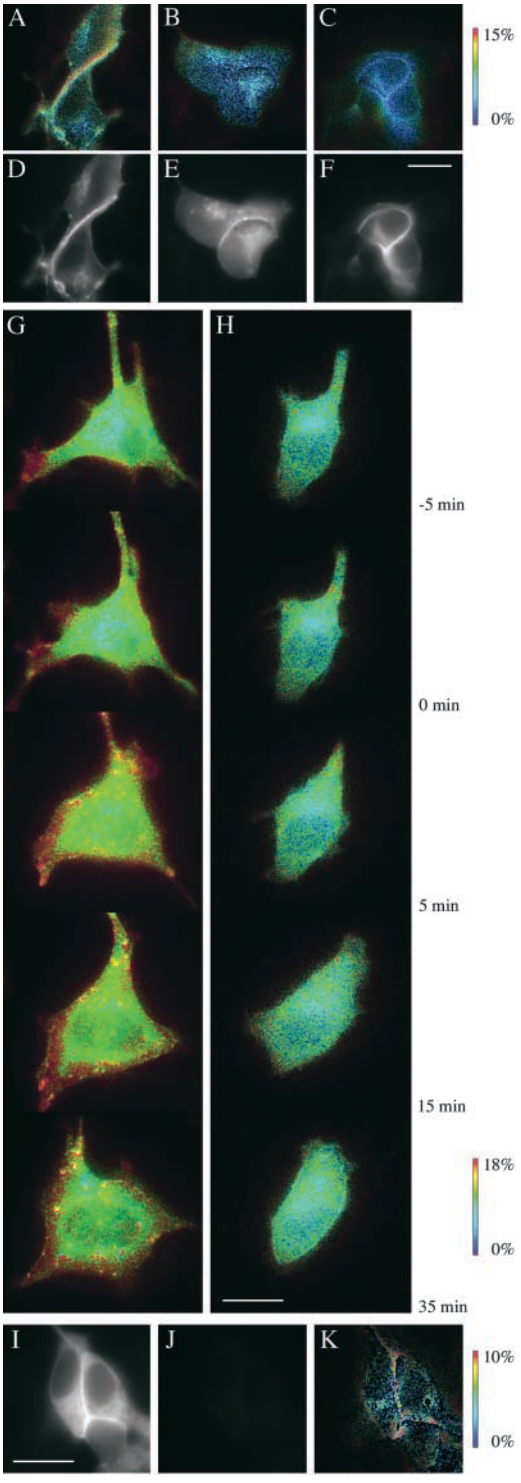

Figure 3. **L1CD–ankyrin$_B$ interactions as assessed by quantitative FRET microscopy.** (A–H) Three fluorescent images of 293 cells expressing L1-CFP and Venus-ankyrin$_B$ were obtained, and FRET^E was calculated and displayed using quantitative pseudocolor (see Materials and methods). (A–F) 293 cells were cotransfected with Venus-ankyrin$_B$ and wild-type L1-CFP (A and D), Venus-ankyrin$_B$ and L1$_{Y1229H}$-CFP (B and E), or Venus-ankyrin$_B$ and L1$_{S1224L}$-CFP (C and F). Shown are FRET^E (A–C) and CFP images (D–F) of the cells. (G and H) Time-lapse images of FRET^E in living cells expressing wild-type L1-CFP and Venus-ankyrin$_B$. Anti-L1-CAM antibody (G) or anti-L1CD antibody (H) was added to the culture medium at 0 min. (I–K) 293 cells were transfected with L1-CFP and Venus-ankyrin$_B$, and FRET^E was measured using the acceptor photobleaching method. Shown are Venus images before (I) and after (J) bleaching, and a FRET^E image (K) given as $1 - I_{da}/I_d$, where I_{da} and I_d are CFP image intensities before and after the acceptor bleaching, respectively. Bars, 20 μm.

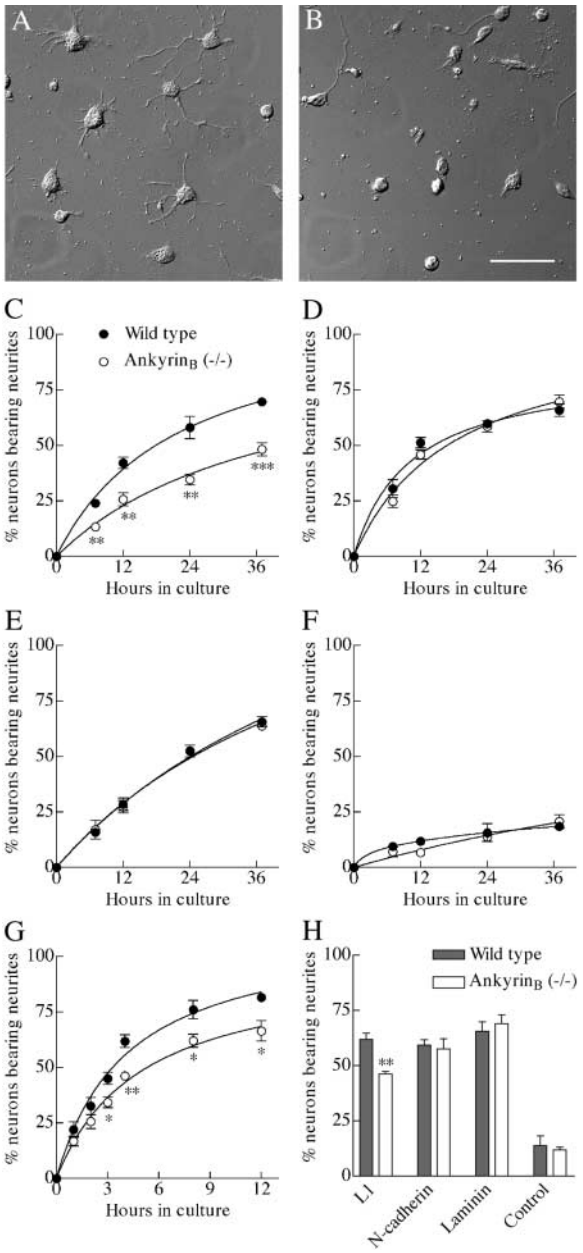

Figure 4. **Ankyrin$_B$ is involved in L1-stimulated neurite initiation.** (A and B) DIC images of cerebellar granule cells derived from wild-type mice (A) or ankyrin$_B^{(-/-)}$ mice (B). The cells have been cultured on an L1-Fc substrate for 20 h. Bar, 50 μm. (C–F) Neurite initiation from cerebellar granule cells plated on L1-Fc (C), N-cadherin–Fc (D), laminin (E), or a control substrate coated with anti-Fc antibody but no CAM-Fc (F). The percentage of neurons bearing neurites was plotted against hours in culture. Neurons from ankyrin$_B^{(-/-)}$ mice (open circles) and their wild-type littermates (closed circles) were analyzed. (G) L1-stimulated neurite initiation from wild-type DRG neurons (closed circles) and ankyrin$_B^{(-/-)}$ DRG neurons (open circles). (H) DRG neurons were cultured for 4 h on the indicated substrates, and the percentage of neurons bearing neurites was quantified. Each value is from four determinations involving >200 neurons. *, $P < 0.05$; **, $P < 0.01$; ***, $P < 0.001$; compared with wild-type neurons under the same culture conditions.

Table I. **Characteristics of ankyrin$_B^{(-/-)}$ cerebellar granule cells**

Genotype	Substrate	Surviving cells[a] ($n = 4$)	Zic-positive cells[b] ($n = 4$)	Neurite length at 37 h after plating ($n = 200$)
		%	%	μm
Wild type	L1-Fc	95.5 ± 1.9	89.5 ± 1.4	86.9 ± 3.8
	N-cadherin-Fc	94.5 ± 0.6	90.9 ± 1.7	81.6 ± 4.0
	Laminin	92.0 ± 1.3	90.8 ± 0.9	67.9 ± 3.4
	Control	84.0 ± 2.9	ND	ND
Ankyrin$_B^{(-/-)}$	L1-Fc	95.7 ± 1.7	91.0 ± 1.9	85.0 ± 3.6
	N-cadherin-Fc	97.0 ± 0.7	91.7 ± 1.0	78.8 ± 3.7
	Laminin	90.9 ± 1.5	92.5 ± 2.1	65.4 ± 2.8
	Control	89.7 ± 3.8	ND	ND

ND, not determined.
[a]Cell viability was determined by trypan blue staining.
[b]Zic is a marker for granule cells in the cerebellum (Aruga et al., 1994).

tiate neurites on an L1 substrate, but not on the other two substrates. Considering the level of background neurite initiation on a control substrate coated with anti-Fc antibody but no CAM-Fc (Fig. 4, F and H), the loss of ankyrin$_B$ expression resulted in 30–50% decrease in L1-dependent neurite initiation. In contrast, the length of neurites did not depend on ankyrin$_B$ expression on any of the substrates tested (Table I and Table II), indicating that ankyrin$_B$ is not involved in neurite elongation. The loss of ankyrin$_B$ expression did not affect viability of the neurons, and the populations of the surviving neurons did not depend on the substrates tested (Table I and Table II). We also compared ankyrin$_G^{(-/-)}$ cerebellar granule cells with wild-type neurons, but there was no significant difference in neurite initiation and elongation on any of the substrates tested (Table III).

Next, we tested whether neurite initiation is affected by overexpression of L1-CAM mutants (L1-CAM$_{\Delta C77}$, L1-CAM$_{Y1229H}$, and L1-CAM$_{S1224L}$) in a dominant-negative manner. To ensure a high level expression of transfected L1-CAM in DRG neurons before neurite initiation, we established a culture system in which neurite initiation could be delayed up to ~24 h after gene transfer. Transfected neurons that had been cultured for 17 h on a substrate coated with anti-Fc antibody were stimulated by adding soluble CAM-Fc chimera that would bind to the anti-Fc antibody and serve as a neurite growth–promoting substrate. Then, neurite initiation was assessed after an additional 4-h incubation. Both L1-Fc and N-cadherin–Fc stimulated neurite initiation in a dose-dependent manner (Fig. 5, A and B). Based on this result, neurite initiation induced by 12 nM CAM-Fc was quantified from DRG neurons that had been transfected with human L1-CAM cDNA. Expression of the transgene was confirmed by immunocytochemistry using the mAb 5G3 that specifically recognizes human L1-CAM (Wolff et al., 1988). The level of overexpression of the transgene was estimated by indirect immunofluorescence using anti-L1CD as a primary antibody. Because the L1CD is completely conserved in mammals at the amino acid level, this antibody should bind equally to transfected human wild-type L1-CAM and endogenous mouse L1-CAM. Fluorescent images of DRG neurons were acquired with a 12-bit CCD camera followed by background subtraction. The L1CD immunoreactivity was quantified by measuring the average fluorescent intensities (0–4095) of pixels within a neuron: 2422 ± 203 in 5G3-positive neurons ($n = 14$) and 176 ± 15 in 5G3-negative neurons ($n = 18$). This result indicated that the level of transfected L1-CAM was >10 times the amount of endogenous L1-CAM, which should be sufficient to exert a dominant-negative effect. As shown in Fig. 5 (C and D), neurons overexpressing any of the L1-CAM mutants had an impaired ability to initiate neurites in response to L1-Fc as compared with those transfected with wild-type L1-CAM. These data, together with our results on ankyrin$_B^{(-/-)}$ neurons, demonstrate that L1CD–ankyrin$_B$ interactions are involved in L1-mediated neurite initiation. The dominant-negative effect of these L1-CAM mutants ap-

Table II. **Characteristics of ankyrin$_B^{(-/-)}$ DRG neurons**

Genotype	Substrate	Surviving cells[a] ($n = 4$)	TrkA-positive cells ($n = 4$)	TrkC-positive cells ($n = 4$)	Neurite length at 12 h after plating ($n = 91$–100)
		%	%	%	μm
Wild type	L1-Fc	93.9 ± 0.9	48.7 ± 3.8	28.8 ± 2.2	129.4 ± 7.5
	N-cadherin-Fc	94.1 ± 1.1	49.7 ± 3.5	31.2 ± 5.3	175.9 ± 8.9
	Laminin	90.7 ± 2.4	49.5 ± 2.6	32.4 ± 5.2	183.1 ± 12.8
	Control	85.8 ± 0.9	51.1 ± 4.4	34.1 ± 3.6	28.8 ±1.5
Ankyrin$_B^{(-/-)}$	L1-Fc	92.3 ± 1.2	47.3 ± 3.9	29.7 ± 1.7	120.7 ± 6.9
	N-cadherin-Fc	89.6 ± 1.7	49.4 ± 4.8	34.4 ± 1.4	183.0 ± 8.7
	Laminin	94.4 ± 1.5	45.6 ± 1.9	29.7 ± 2.6	191.1 ± 10.5
	Control	90.6 ± 1.7	48.6 ± 4.8	34.2 ± 1.9	25.2 ± 1.4

[a]Cell viability was determined by trypan blue staining.

Table III. **Neurite initiation and elongation from ankyrin$_G^{(-/-)}$ cerebellar granule cells**

Genotype	Substrate	Neurons bearing neurites at 40 h after plating ($n = 8$)	Neurite length at 40 h after plating ($n = 100$)
		%	μm
Wild type	L1-Fc	71.6 ± 0.1	105.9 ± 6.5
	N-cadherin-Fc	79.5 ± 0.1	88.8 ± 5.7
	Laminin	67.2 ± 0.2	103.7 ± 6.1
Ankyrin$_G^{(-/-)}$	L1-Fc	76.1 ± 0.2	98.2 ± 6.4
	N-cadherin-Fc	76.6 ± 0.1	91.9 ± 5.7
	Laminin	65.5 ± 0.1	99.8 ± 5.9

peared slightly more prominent than the effect of ankyrin$_B$ knockout (Fig. 4 G). This is presumably because the mutations in the ankyrin-binding region of the L1CD may have an additional consequence, e.g., decreased signaling to the MAPK pathway (Thelen et al., 2002).

Because DRG neurons in P0 mice bear neurites in vivo, preparation of the neuronal cultures should have shorn the neurites from their somata. Depending on an enzyme used to dissociate the neural tissues, the proximal short segment of a neurite remained connected with its soma (unpublished data). The presence of such remnants of neurites would affect the percentage of neurons bearing neurites, used as an indicator of neurite initiation. However, the dissociation method with dispase II used in the present work completely sheared neurites from their somata, and we did not observe any neurons that bore neurites immediately after the dissociation. Therefore, our data represent the ability of neurons to "re-initiate" neurites in response to CAM ligation.

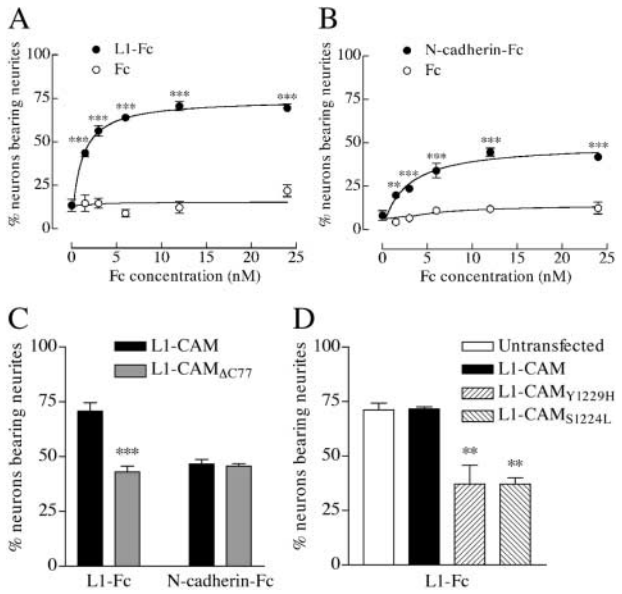

Figure 5. **L1-mediated neurite initiation is suppressed by overexpression of L1-CAM mutants that do not interact with ankyrin$_B$.** (A and B) The CAM-Fc dose–response curves for neurite initiation from DRG neurons. Neurons were cultured on an anti-Fc antibody substrate for 14 h after lipofection. Neurite initiation was assessed at 4 h after addition of L1-Fc (closed circles) or Fc (open circles) at indicated concentrations. CAM-Fc (A) or N-cadherin–Fc (B) stimulated neurite initiation in a dose-dependent manner. Each value is from four determinations involving >200 neurons. **, $P < 0.01$; ***, $P < 0.001$; compared with Fc-treated neurons. (C and D) DRG neurons were transfected with wild-type L1-CAM or L1-CAM mutants, and neurite initiation stimulated by 12 nM of L1-Fc or N-cadherin–Fc was quantified as described above. Overexpression of L1-CAM$_{\Delta C77}$ (C), L1-CAM$_{Y1229H}$ (D), or L1-CAM$_{S1224L}$ (D) impaired L1-stimulated neurite initiation as compared with overexpression of wild-type L1-CAM. As another control, L1-stimulated neurite initiation from untransfected neurons was quantified (D). N-cadherin–stimulated neurite initiation was not affected by L1-CAM$_{\Delta C77}$ overexpression (C). **, $P < 0.01$; ***, $P < 0.001$; compared with neurons overexpressing wild-type L1-CAM.

Ankyrin$_B$ mediates L1-CAM coupling with retrograde F-actin flow in membranous protrusions surrounding the soma

In the process of neuritogenesis, DRG neurons always formed membranous protrusions surrounding the soma (Fig. 6 A), which were termed the perisomatic lamellae and filopodia in this paper. Dynamic properties of F-actin in these perisomatic structures were investigated by fluorescent speckle microscopy, in which low concentrations of fluorescently labeled phalloidin were used to generate fiducial marks (speckles) on F-actin (Schaefer et al., 2002a). As shown in Fig. 6 (B and C), F-actin moved toward the soma. The speed of retrograde F-actin flow did not depend on ankyrin$_B$ expression: 6.3 ± 0.2 μm/min ($n = 48$) in 12 wild-type neurons and 6.1 ± 0.2 μm/min ($n = 56$) in 14 ankyrin$_B^{(-/-)}$ neurons.

To test whether ankyrin$_B$ associates with retrograde F-actin flow, the movement of Venus-ankyrin$_B$ expressed in DRG neurons was monitored by time-lapse fluorescent microscopy. As shown in Fig. 6 (D and E), ankyrin$_B$ formed clusters of various sizes in the perisomatic lamellae and filopodia. Smaller clusters of ankyrin$_B$ often moved toward the soma, whereas larger clusters tended to be stationary. The representative movement of a small ankyrin$_B$ cluster in the perisomatic filopodia is shown in Fig. 6 F. We simultaneously acquired differential interference contrast (DIC) images to exclude the possibility that the observed ankyrin$_B$ movement was due to filopodial retraction. An ankyrin$_B$ cluster was often found in a bulbous structure in the filopodia (Fig. 6 F, DIC images). The speed of retrograde ankyrin$_B$ flow was 5.7 ± 0.3 μm/min ($n = 24$; eight neurons), which was comparable with that of F-actin flow. Treatment of neurons with cytochalasin D reversibly blocked the retrograde ankyrin$_B$ flow (Fig. 6, G–I). These results indicate that ankyrin$_B$ associates with retrograde F-actin flow in the perisomatic structures, although we could not image the movement of ankyrin$_B$ clusters in the perisomatic lamellae due to high background fluorescent signals. We

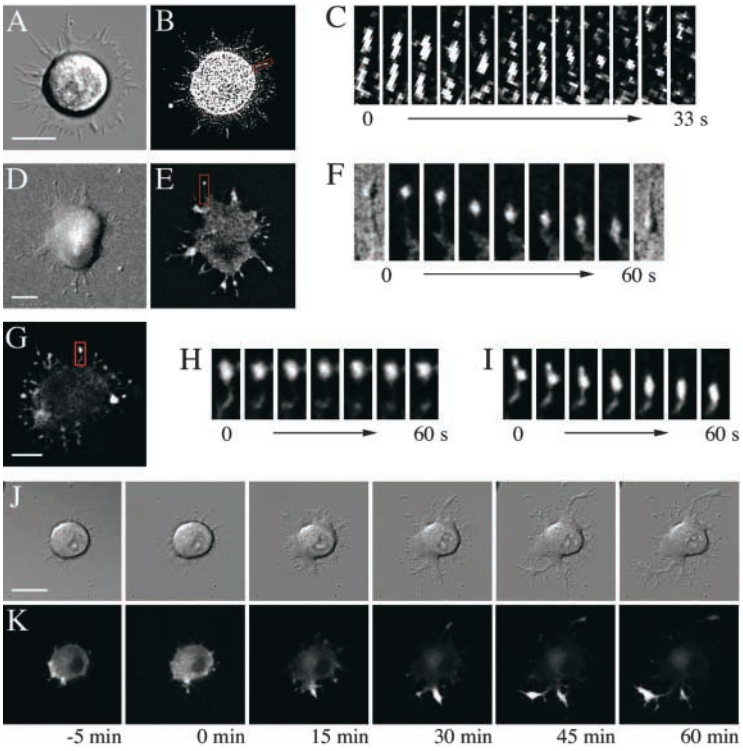

Figure 6. **Dynamics of F-actin and ankyrin$_B$ in the perisomatic lamellae and filopodia of DRG neurons.** (A–C) F-actin dynamics in the perisomatic lamellae and filopodia was analyzed by fluorescent speckle microscopy. Shown are a DIC image (A) and an image of speckles generated on F-actin (B). (C) Time sequence of the speckle movement in the area of interest indicated in B in red. (D–F) Ankyrin$_B$ dynamics in a DRG neuron. Shown are a DIC image (D) and a fluorescent image of Venus-ankyrin$_B$ (E). (F) Time sequence of the Venus-ankyrin$_B$ movement in the area of interest indicated in E in red. DIC images at 0 and 60 s are also shown. (G–I) Reversible inhibition of retrograde ankyrin$_B$ flow by cytochalasin D. (H) Time-lapse images of Venus-ankyrin$_B$ in the perisomatic filopodium surrounded by the red rectangle in G in the presence of 5 μg/ml cytochalasin D. (I) Resumed movement of Venus-ankyrin$_B$ in the same filopodium after removal of cytochalasin D. (J and K) Time-lapse DIC (J) and fluorescent (K) images of a DRG neuron showing the process of neurite initiation and subcellular distribution of Venus-ankyrin$_B$. Neurons that had been cultured on a substrate coated with anti-Fc antibody were stimulated with L1-Fc at 0 min. Bars, 10 μm.

also tested whether spectrin mediates ankyrin$_B$ coupling with F-actin flow, using an ankyrin$_B$ mutant that had a single amino acid substitution, A1000P, in the spectrin-binding domain and did not interact with spectrin (unpublished data). When expressed in DRG neurons, this ankyrin$_B$ mutant was less likely to form clusters than wild-type ankyrin$_B$, and the mutant clusters did not show the retrograde directional movement in the perisomatic filopodia. This suggests that ankyrin$_B$ associates with F-actin flow via spectrin.

Interestingly, neurons cultured on an L1-Fc substrate for 2 h were more likely to have large stationary ankyrin$_B$ clusters than those cultured on an N-cadherin–Fc substrate: 43.6 ± 4.8% (n = 4) out of >200 neurons on L1-Fc had such clusters, compared with 25.1 ± 3.1% (n = 4) on N-cadherin–Fc. Endogenous ankyrin$_B$ also formed large clusters colocalizing with endogenous L1-CAM in the perisomatic lamellae of DRG neurons on an L1-Fc substrate (Fig. 7, A–C). These results, together with the FRET data (Fig. 3), suggested to us that L1ED ligation induced the formation of a molecular complex involving F-actin, ankyrin$_B$, L1-CAM, and an immobile extracellular substrate (L1-Fc in this case). Such a complex would be able to transmit traction force generated by F-actin to the substrate, leading to the formation of neurites.

This hypothesis was supported by longer term time-lapse imaging of Venus-ankyrin$_B$–transfected neurons (Fig. 6, J and K) and by FRET imaging of neurons (Fig. 8). L1-stimulated neurite initiation preferentially occurred at the site of large stationary ankyrin$_B$ clusters (Fig. 6, J and K; neurites at the bottom), although some neurites were formed independent of ankyrin$_B$ clustering (Fig. 6, J and K; neurites at the top). Analyses of 11 neurons stimulated with L1-Fc revealed that 14 of 17 neurites were formed at the site of stationary ankyrin$_B$ clusters, whereas only 4 of 20 neurites from 11 neurons stimulated with N-cadherin–Fc were formed at the site of such clusters. FRET microscopy of fixed neurons indicated that the L1CD interacted with ankyrin$_B$ at the site of large ankyrin$_B$ clusters in the perisomatic lamellae if neurons had been stimulated with L1-Fc, but not with N-cadherin–Fc (Fig. 8, A–G). Quantitative analyses gave the following results: 20 of 68 (29.4%) ankyrin$_B$ clusters in the perisomatic lamellae of L1-treated neurons showed FRET^E >8%, whereas only 1 of 46 (2.1%) ankyrin$_B$ clusters of N-cadherin–treated neurons showed FRET^E >8%. We also found that growth cones rarely (4.5%; 2 of 44 growth cones with strong Venus-ankyrin$_B$ expression) showed FRET^E >8%

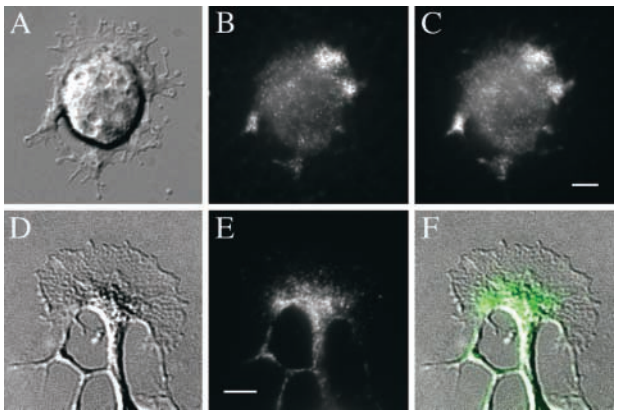

Figure 7. **Immunofluorescent images of DRG neurons showing the localization of endogenous ankyrin$_B$ and endogenous L1-CAM.** (A–C) DIC (A), ankyrin$_B$ (B), and L1-CAM (C) images of a neuron cultured on an L1-Fc substrate for 2 h. (D–F) DIC (D) and ankyrin$_B$ (E) images of a neuron cultured on an L1-Fc substrate for 6 h. The two images were superimposed with ankyrin$_B$ colored in green (F). Bars, 5 μm.

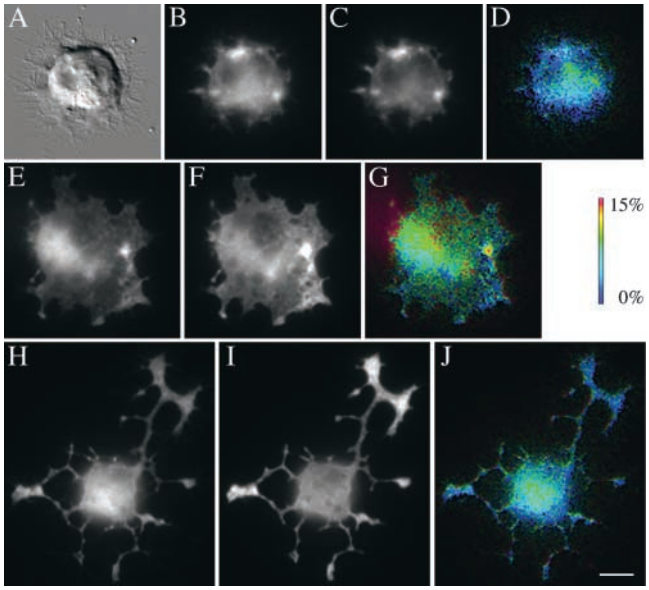

Figure 8. **L1-CAM interacts with ankyrin$_B$ in the perisomatic lamellae (but not in the growth cones) as assessed by FRET microscopy.** (A–G) DRG neurons expressing L1-CFP and Venus-ankyrin$_B$ were stimulated for 1.5 h with N-cadherin–Fc (A–D) or L1-Fc (E–G). Shown are CFP images (B and E), Venus images (C and F), and FRET^E images displayed using quantitative pseudocolor (D and G). A DIC image (A) indicates that the CFP and Venus clusters (B and C) are localized to the perisomatic lamellae. (H–J) An L1-CFP image (H), a Venus-ankyrin$_B$ image (I), and a FRET^E image (J) of a DRG neuron that has been stimulated with L1-Fc for 3 h to induce neurite initiation and elongation. Bar, 10 μm. We defined true FRET as multiple pixels (at least four neighboring pixels of two lines by two rows in the original 8 × 8 binned image) exhibiting FRET^E >8%. Isolated single pixels or a line of single pixels exhibiting FRET^E >8% were considered false positives, as these signals were likely to be due to subpixel misalignment of the three raw images or readout noise from the CCD camera. FRET^E values in the neuronal soma were disregarded because FRET measurements were often affected by fluorescent signals derived from unfocal planes in the thick soma.

even if neurite initiation and elongation had been stimulated by L1-Fc (Fig. 8, H–J). Although the FRET analysis does not exclude the possibility of L1-CAM interaction with ankyrin$_B$ in growth cones, the interaction is unlikely to occur in the peripheral domain because expression of endogenous ankyrin$_B$ was restricted to the central domain in growth cones as assessed by immunocytochemistry (Fig. 7, D–F). Collectively, our results so far strongly suggest that ankyrin$_B$, in response to L1ED ligation, links the L1CD with retrograde F-actin flow in the perisomatic membranous structures, but not in the growth cone peripheral domain.

Direct evidence that endogenous ankyrin$_B$ is involved in L1-CAM coupling with retrograde F-actin flow has been obtained by bead-tracking experiments. As we reported previously (Kamiguchi and Yoshihara, 2001), microbeads coated with either L1-Fc or anti-L1-CAM antibody bound to L1-CAM expressed on the growth cone lamellae and showed retrograde directional movement when coupled with F-actin flow. In the present work, we monitored the movement of beads coated with L1-Fc, anti-L1-CAM antibody, or laminin on the perisomatic lamellae of wild-type or ankyrin$_B^{(-/-)}$ DRG neurons. On either group of neurons, 88–92% of the

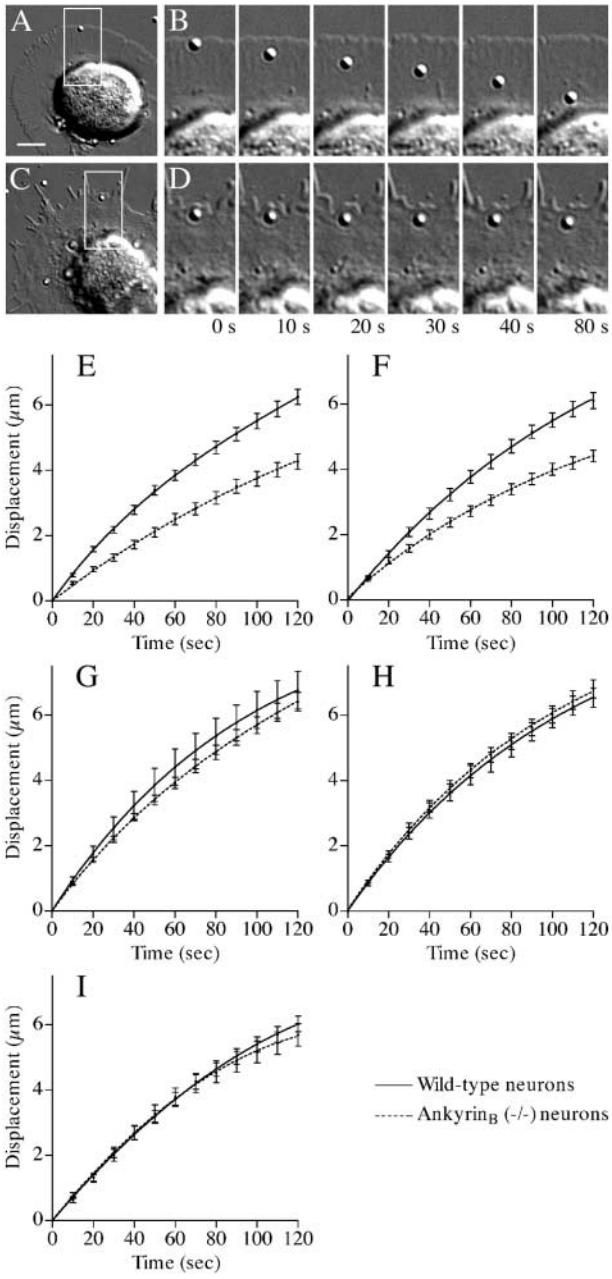

Figure 9. **Ankyrin$_B$ is involved in L1-CAM coupling with retrograde F-actin flow in the perisomatic lamellae, but not in the growth cone lamellae.** (A–D) DIC images of wild-type (A and B) and ankyrin$_B^{(-/-)}$ (C and D) DRG neurons. An L1-Fc–coated bead was placed on the leading edge of a perisomatic lamella with laser tweezers (0 s). (B and D) Time sequence of the bead movement in the area of interest indicated in A and C, respectively. Bar (A and C), 5 μm. (E–I) Cumulative displacement of beads plotted as a function of time. The movement of beads coated with L1-Fc (E and G), anti-L1-CAM antibody (F and H), or laminin (I) was monitored on perisomatic lamellae (E, F, and I) and on growth cone lamellae (G and H). The bead behavior was analyzed on DRG neurons derived from ankyrin$_B^{(-/-)}$ mice (dashed lines) and their wild-type littermates (solid lines). Each set of experiments involved 14–28 beads.

beads showed retrograde directional movement regardless of the coating proteins, whereas the remaining 8–12% showed Brownian motion on the cell surface. On wild-type neurons pretreated with 0.5 μg/ml cytochalasin D, none of 25 L1-

Fc–coated beads that had bound to the cell surface showed retrograde directional movement, indicating that this type of bead movement is driven by F-actin flow. To assess the coupling efficiency of L1-CAM with F-actin flow, we measured the speed of retrograde bead movement. Note that the speed of F-actin flow does not depend on ankyrin$_B$ expression as described in the previous paragraph. The movement of beads coated with either L1-Fc or anti-L1-CAM antibody on ankyrin$_B^{(-/-)}$ neurons was significantly retarded compared with that on wild-type neurons (Fig. 9, A–F), indicating that ankyrin$_B$ is required for the full engagement of L1-CAM with retrograde F-actin flow in the perisomatic lamellae. As a control, the loss of ankyrin$_B$ expression did not affect the movement of laminin-coated beads (Fig. 9 I). The partial slippage between L1-CAM and F-actin flow in ankyrin$_B^{(-/-)}$ neurons indicated the existence of other clutch molecules. One candidate is a member of the ERM (ezrin-radixin-moesin) family, an actin-binding protein that has recently been demonstrated to interact with the Arg-Ser-Leu-Glu (RSLE)–containing region in the L1CD (Dickson et al., 2002). To explore this possibility, we generated cDNA constructs of wild-type and RSLE-minus human L1-CAM tagged to GFP, and transfected mouse DRG neurons with each construct. Neurons expressing the transgene were identified by GFP fluorescence, and a microbead coated with 200 μg/ml 5G3 was placed on the tip of a perisomatic filopodium. Out of the 26 beads tested on the perisomatic filopodia expressing wild-type human L1-CAM, 12 beads moved retrogradely at 2.4 ± 0.2 μm/min. In contrast, the beads (n = 27) never showed retrograde directional movement on the perisomatic filopodia expressing RSLE-minus human L1-CAM. Therefore, a member of the ERM family might be another component of the clutch module that regulates L1-based neurite initiation.

Our result that ankyrin$_B$ was not required for neurite elongation led us to test for the involvement of ankyrin$_B$ in L1-CAM coupling with F-actin flow in growth cone lamellae. As expected, the loss of ankyrin$_B$ expression did not affect retrograde movement of beads coated with either L1-Fc or anti-L1-CAM antibody on growth cone lamellae (Fig. 9, G and H). This was also consistent with our result that ankyrin$_B$ did not interact with the L1CD in the growth cone peripheral domain. Collectively, the data indicate that neurons change components of the clutch module during neurite growth and that ankyrin$_B$ acts as a clutch component only before neurite formation.

Discussion

The clutch hypothesis states that cell motility is controlled by regulated engagement between retrograde F-actin flow and CAMs bound to an immobile substrate (Mitchison and Kirschner, 1988). Although many pieces of evidence for this hypothesis have been reported, the question has not been answered as to what molecules constitute the clutch module (Jay, 2000). With respect to CAM–cytoskeletal linkages, integrins are by far the best-studied family of CAMs. Focal adhesion proteins are obvious candidates for the clutch module that connects integrins with F-actin flow. The cytoskeletal linkage via focal adhesion proteins, such as talin and vinculin, has been implicated in cell motility and neurite growth (Nuckolls et al., 1992; Varnum-Finney and Reichardt, 1994; Sydor et al., 1996). Furthermore, it has been reported that focal adhesions, as labeled with GFP-integrin chimera, exhibit nonmotile and motile states coordinated with cell migration, suggesting the existence of a molecular clutch that alternates between these states (Smilenov et al., 1999). However, it remains to be determined what molecules connect CAMs with F-actin flow in such a regulated manner. The most important aspect of our research is the direct demonstration that ankyrin$_B$ mediates L1-CAM coupling with F-actin flow. In addition, we provide the following results that support the idea that ankyrin$_B$ constitutes the clutch module regulating L1-mediated neurite initiation (Fig. 10): (1) ankyrin$_B$ showed retrograde movement that was associated with F-actin flow; (2) in response to L1ED ligation by an immobile substrate, ankyrin$_B$ interacted with the L1CD and formed stationary clusters; (3) neurite initiation preferentially occurred at the site of stationary ankyrin$_B$ clusters; and (4) neurite initiation was impaired by loss of L1CD–ankyrin$_B$ interactions.

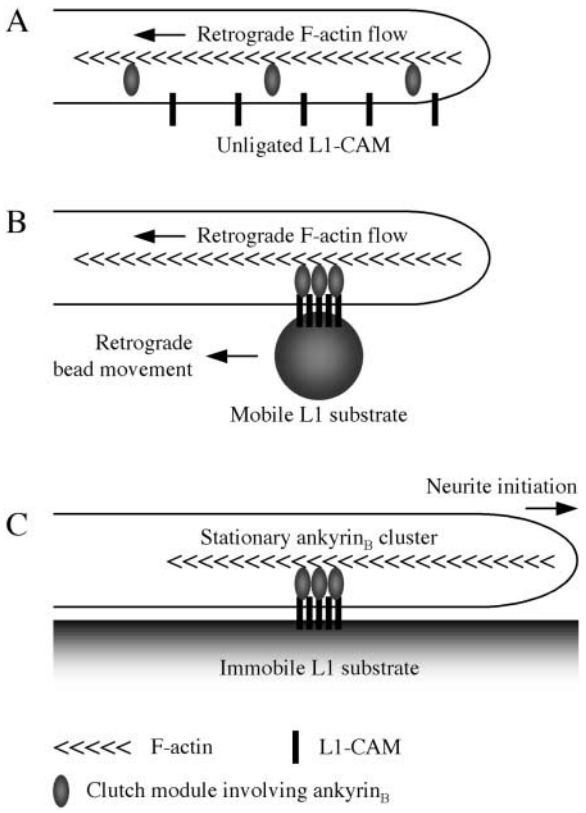

Figure 10. **A model of the clutch mechanism that regulates L1-mediated neurite initiation.** (A) In the perisomatic membranous structure, ankyrin$_B$ indirectly associates with retrograde F-actin flow via spectrin, but does not bind to unligated L1-CAM. (B) Ligation of neuronal L1-CAM with a mobile L1 substrate (e.g., an L1-Fc–coated bead) results in L1CD–ankyrin$_B$ binding and clustering of the clutch module. In this situation, the clutch is engaged and the bead is pulled toward the soma by F-actin flow. (C) When neuronal L1-CAM is ligated with an immobile L1 substrate, the traction force transmitted via the clutch module drives neurite protrusion by pulling the immobile substrate backward. In this situation, the ankyrin$_B$ cluster is stationary in respect to the substrate.

Another important topic in this paper is the differences between ankyrin$_G$ and ankyrin$_B$: (1) coexpression of the L1CD with ankyrin$_G$ is sufficient for their interaction, whereas the L1CD binds to ankyrin$_B$ in response to L1ED ligation; and (2) L1-CAM binding to ankyrin$_B$ (but not to ankyrin$_G$) is involved in neurite initiation. This suggests that ankyrin$_B$ collaborates with L1-CAM in dynamic cell functions, whereas ankyrin$_G$ may be involved in rather static adhesion. The idea that different forms of ankyrins have distinct functional significance could be supported by a recent report (Gil et al., 2003). They showed that the ankyrin-binding activity of the L1CD is required for its interactions with static components of the cytoskeleton in ND-7 neuroblastoma hybrid cells, and also that the binding activity inhibits retrograde L1-CAM movement on the cell surface. Although not identified in their report, some form of ankyrins expressed in ND-7 cells should mediate such static interactions, which is in striking contrast to the role of ankyrin$_B$ demonstrated in our paper. It is likely that a large number of ankyrin isoforms play diverse roles in different cell types and at different developmental stages.

As has been shown in neurofascin–ankyrin binding (Garver et al., 1997), phosphorylation of Y^{1229} in the L1CD might be responsible for the lack of ankyrin$_B$ interactions with nonligated L1-CAM. However, the ankyrin recruitment assay using *Drosophila* S2 cells showed that ankyrin recruitment was dramatically reduced, but still limited to cell contact sites when the corresponding tyrosine residue of neuroglian, a *Drosophila* homologue of L1-CAM, was mutated to a phenylalanine (Hortsch et al., 1998a). We also obtained a similar result with L1-CAM$_{Y1229F}$-expressing 293 cells (unpublished data). Therefore, another mechanism must be responsible for the outside-in regulation of L1CD–ankyrin$_B$ binding. There are at least five other phosphorylation sites in the L1CD (Kamiguchi and Lemmon, 1997; Schaefer et al., 1999, 2002b), but none of the amino acid substitutions of these phosphorylation sites affected the selective recruitment of ankyrin$_B$ to cell contact sites (unpublished data). Alternatively, a conformational change in the L1CD induced by oligomerization of the L1ED (Silletti et al., 2000) could be the mechanism, as proposed by Jefford and Dubreuil (2000), but further research will be required to solve this problem.

Materials and methods

Antibodies

Rabbit antisera against human L1-CAM, rat L1-CAM, and L1CD were provided by Dr. Vance Lemmon (Case Western Reserve University, Cleveland, OH). These antisera have been described previously (Hlavin and Lemmon, 1991; Schaefer et al., 1999; Long et al., 2001). Rabbit anti-Zic antibody was a gift of Dr. Jun Aruga (RIKEN Brain Science Institute, Saitama, Japan; Aruga et al., 1994). Mouse anti–human L1-CAM antibody (5G3) was purchased from BD Biosciences, mouse anti-ankyrin$_B$ antibody from Zymed Laboratories, rabbit antibodies against TrkA and TrkC from CHEMICON International, and Alexa®-conjugated secondary antibodies from Molecular Probes, Inc.

cDNA constructs

The generation of cDNA constructs is explained in detail in the supplemental Materials and methods section (available at http://www.jcb.org/cgi/content/full/jcb.200303060/DC1). In brief, the pcDNA3-based expression plasmids (Invitrogen), which contain a cDNA encoding for the neuronal form or its mutant forms of human L1, were generated using the site-directed mutagenesis kit (CLONTECH Laboratories, Inc.). The plasmids containing L1-CAM$_{\Delta C77}$ cDNA have been described previously (Kamiguchi and Lemmon, 1998). The pECFP-N1 vector (CLONTECH Laboratories, Inc.) encoding for L1-CFP, in which CFP is tagged to the COOH terminus of human L1-CAM via a multiple (GGS/TG) amino acid linker, was generated by PCR. Similarly, the vector encoding for Venus-ankyrin$_B$, in which Venus is tagged to the NH_2 terminus of human ankyrin$_B$, was generated by PCR. The linker sequences in both L1-CFP and Venus-ankyrin$_B$ were optimized based on FRET^E measurements in transfected 293 cells: L1-(GGSGGGTGGGSG)-CFP and Venus-(GSGGGS)-ankyrin$_B$. Human L1-CAM cDNA was provided by Dr. Vance Lemmon, and Venus cDNA by Dr. Atsushi Miyawaki (RIKEN Brain Science Institute).

Cell culture

The cerebelli and DRGs dissected from P0 mice were dissociated as described previously (Nakai and Kamiguchi, 2002), and were plated on a dish coated with 9 μg/cm^2 laminin (Life Technologies) or CAM-Fc. Production of CAM-Fc, which consists of the whole extracellular domain of a CAM (chick L1-CAM or chick N-cadherin) and the Fc region of human IgG, was performed as described previously (Kamiguchi and Yoshihara, 2001). CAM-Fc–coated dishes were prepared by sequential coating with 0.1 mg/ml poly-D-lysine (70–150 kD; Sigma-Aldrich), 40 μg/ml anti-Fc antibody (Sigma-Aldrich), and CAM-Fc. The N-cadherin–Fc cDNA construct was a gift of Dr. Patrick Doherty (Guy's Hospital, London, UK). Neurons were cultured in serum-free media with essential supplements as described previously (Nakai and Kamiguchi, 2002).

HEK 293 cells (American Type Culture Collection) were seeded on a dish coated with 6 μg/cm^2 fibronectin (Life Technologies) and cultured in RPMI 1640 medium supplemented with 10% FBS.

The cultures were maintained in a humid atmosphere of 95% air, 5% CO_2 at 37°C. For live-cell imaging, 293 cells were cultured in Leibovitz's L-15 medium (Life Technologies), and DRG neurons in L-15 supplemented with N-2 (Life Technologies) and 50 ng/ml NGF (Promega), in a humid atmosphere of 100% air at 37°C on a microscope stage.

Transfection

HEK 293 cells were transfected with expression plasmids using FuGENE™ 6 transfection reagent (Roche) according to the manufacturer's protocol. DRG neurons were transfected with LipofectAMINE™ 2000 (Life Technologies). To allow for high level expression of transgene products before neurite initiation, we used the following protocol: (1) DRG neurons were plated on a dish coated sequentially with poly-D-lysine and anti-Fc antibody and incubated for 3 h. (2) The cells were incubated in the presence of DNA–LipofectAMINE™ 2000 complexes for 2 h according to the manufacturer's protocol. (3) After an additional 12-h incubation, CAM-Fc was added to the culture medium to stimulate neurite growth.

Immunocytochemistry

HEK 293 cells were fixed with 4% formaldehyde in PBS for 20 min, blocked with 10% horse serum in PBS for 1 h, and incubated with rabbit anti–human L1-CAM antiserum (1:5,000 dilution) for 1 h at 37°C. L1-CAM was labeled by incubating the cells with 10 μg/ml Alexa 594®–conjugated anti–rabbit IgG for 1 h at RT.

Neurons were fixed with 4% formaldehyde and blocked with 10% horse serum. In some cases, the cells were permeabilized with 0.1% Triton X-100. The following primary antibodies were used: 10 μg/ml 5G3, anti-L1CD antiserum (1:10,000 dilution), anti-Zic antibody, 2 μg/ml anti-TrkA antibody, 1 μg/ml anti-TrkC antibody, and 1 μg/ml anti-ankyrin$_B$ antibody. Expression of the proteins was visualized with 10 μg/ml Alexa®-conjugated secondary antibodies.

Neurite growth assay

Neurite-bearing neurons were defined as those that possess cellular processes longer than the diameter of the soma. Included in this paper was a neuron in isolation whose neurites did not contact other cells or neurites. Neurite initiation was assessed by calculating the percentage of neurons bearing neurites. The length of neurites was measured as described previously (Kamiguchi and Yoshihara, 2001).

Confocal microscopy

Images of 293 cells were taken with a confocal imaging system (Radiance 2000; Bio-Rad Laboratories) attached to a microscope (Eclipse TE300; Nikon), using an argon/krypton laser (488 and 568 nm) and a 100× Plan

Apochromat (NA 1.4) objective lens. Pinhole settings were chosen to give single optical sections of 0.6 μm in thickness.

FRET microscopy

To measure FRET^E, three fluorescent images of a cell expressing CFP and YFP (Venus) were acquired in the same order in all experiments through (1) a FRET filter set (excitation 440/21 nm, emission 545/35 nm); (2) a CFP filter set (excitation 440/21 nm, emission 480/30 nm); and (3) a YFP filter set (excitation 500/25 nm, emission 545/35 nm). A single dichroic mirror was used with all three filter sets. The images were acquired with a 12-bit digital CCD camera (CoolSNAP HQ™; Roper Scientific) and a microscope (Axiovert S100; Carl Zeiss MicroImaging, Inc.) using a 100× Plan Apochromat (NA 1.4) objective lens. Exposure time and binning (4 × 4 or 8 × 8) were adjusted so that pixel intensity values were 20–80% saturation in the three channels. A background image was subtracted from each raw image before carrying out FRET calculations.

Quantitative FRET measurements were performed as described previously (Gordon et al., 1998). In brief, corrected FRET (FRET^C) was calculated on a pixel-by-pixel basis for the entire image by subtracting the cross-talks as follows: $FRET^C = I_{FRET} - (0.33 \times I_{CFP}) - (0.05 \times I_{YFP})$, where I_{FRET}, I_{CFP}, and I_{YFP} are image intensities under the FRET, CFP, and YFP filter sets, respectively. 0.33 and 0.05 are the fractions of CFP bleed-through and YFP cross-excitation, respectively, through the FRET filter channel. These coefficients were rounded up from average cross-bleed values determined in cells expressing only CFP- or YFP-tagged constructs alone. Then, FRET^E was calculated by using the following equation: $FRET^E = FRET^C/(I_{CFP} + FRET^C)$. FRET^E images were displayed in a pseudocolor mode (24-bit intensity-modulated display mode) using MetaFluor® version 4.6 (Universal Imaging Corp.).

Fluorescent speckle microscopy

F-actin dynamics was visualized by fluorescent speckle microscopy (Schaefer et al., 2002a). Low concentrations of Alexa® 594–conjugated phalloidin (Molecular Probes, Inc.) were introduced into DRG neurons by trituration loading (Sydor et al., 1996). In brief, DRGs were treated with 0.25% trypsin-EGTA (Life Technologies) at 37°C for 30 min, and triturated using the p20 micropipetman (~150 strokes) in 20 μl of 10 μM Alexa® 594 phalloidin in Leibovitz's L-15 medium. The dissociated cells were plated and cultured in L-15 supplemented with N-2, NGF, and 750 μg/ml BSA. Fluorescent images were acquired every 3 s at the exposure of ~1 s with a CCD camera (ORCA-ER; Hamamatsu Photonics). Contrast of speckles was enhanced by processing the images with the smoothing A and shappen B spatial filters using AquaCosmos version 2.0 (Hamamatsu Photonics).

Imaging of ankyrin$_B$ dynamics

Time-lapse images of DRG neurons expressing Venus-ankyrin$_B$ were acquired with a CCD camera coupled to a blue-enhanced Gen IV intensifier (I-PentaMAX; Roper Scientific) and processed with two-dimensional deconvolution using MetaMorph® version 4.6 (Universal Imaging Corp.).

Laser tweezers

Coating of 800-nm-diam silica beads was performed as described previously (Kamiguchi and Yoshihara, 2001), except that protein A–conjugated beads were incubated with either 10 μg/ml L1-Fc or anti-rat L1-CAM antiserum (1:500 dilution). Laminin-coated beads were prepared as described previously (Kuhn et al., 1995). In brief, a 1% (wt/vol) aqueous solution of 800-nm-diam silica beads with COOH functional groups (Micromod) was mixed with an equal volume of 20 mg/ml carbodiimide in sodium phosphate buffer for 4 h at RT. After washes, the beads were suspended in borate buffer (pH 8.5) and incubated with 50 μg/ml laminin overnight at RT. The beads were blocked with 0.1 M ethanolamine and 7.5 mg/ml BSA and stored in PBS at 4°C. As described previously (Kamiguchi and Yoshihara, 2001), we used the laser optical trap system to place a bead on the leading edge of neuronal lamellae.

Image processing

Size, brightness, and contrast of digital images were adjusted minimally, and montages were assembled using Adobe Photoshop® 6.0.

Statistics

Data were expressed as the mean ± SEM. Statistical analyses were performed using Prism version 3.0a (GraphPad Software). A comparison between two groups was performed by an unpaired *t* test, and a comparison among three or more groups by one-way ANOVA followed by Tukey's post test. P values <0.05 were judged statistically different.

Online supplemental material

The generation of cDNA constructs is explained in detail in the supplemental Materials and methods section, available at http://www.jcb.org/cgi/content/full/jcb.200303060/DC1.

We are grateful to Drs. J. Aruga, P. Doherty, V. Lemmon, and A. Miyawaki for providing DNA constructs and antibodies. We also thank Dr. A. Miyawaki for technical advice on FRET microscopy.

This work was partially supported by Grant-in-Aid for Scientific Research of Japan Society for the Promotion of Science (13680857) and a Health and Labor Sciences Research Grant on research of specific diseases "Congenital Hydrocephalus" (H14-SD-17) to H. Kamiguchi.

Submitted: 10 March 2003
Accepted: 15 October 2003

References

Aruga, J., N. Yokota, M. Hashimoto, T. Furuichi, M. Fukuda, and K. Mikoshiba. 1994. A novel zinc finger protein, zic, is involved in neurogenesis, especially in the cell lineage of cerebellar granule cells. *J. Neurochem.* 63:1880–1890.

Bennett, V., and L. Chen. 2001. Ankyrins and cellular targeting of diverse membrane proteins to physiological sites. *Curr. Opin. Cell Biol.* 13:61–67.

Bixby, J.L., and R. Zhang. 1990. Purified N-cadherin is a potent substrate for the rapid induction of neurite outgrowth. *J. Cell Biol.* 110:1253–1260.

Bozyczko, D., and A.F. Horwitz. 1986. The participation of a putative cell surface receptor for laminin and fibronectin in peripheral neurite extension. *J. Neurosci.* 6:1241–1251.

Dahme, M., U. Bartsch, R. Martini, B. Anliker, M. Schachner, and N. Mantei. 1997. Disruption of the mouse L1 gene leads to malformations of the nervous system. *Nat. Genet.* 17:346–349.

Dickson, T.C., C.D. Mintz, D.L. Benson, and S.R. Salton. 2002. Functional binding interaction identified between the axonal CAM L1 and members of the ERM family. *J. Cell Biol.* 157:1105–1112.

Faivre-Sarrailh, C., J. Falk, E. Pollerberg, M. Schachner, and G. Rougon. 1999. NrCAM, cerebellar granule cell receptor for the neuronal adhesion molecule F3, displays an actin-dependent mobility in growth cones. *J. Cell Sci.* 112: 3015–3027.

Fransen, E., R. D'Hooge, G. Van Camp, M. Verhoye, J. Sijbers, E. Reyniers, P. Soriano, H. Kamiguchi, R. Willemsen, S.K. Koekkoek, et al. 1998. L1 knockout mice show dilated ventricles, vermis hypoplasia and impaired exploration patterns. *Hum. Mol. Genet.* 7:999–1009.

Garver, T.D., Q. Ren, S. Tuvia, and V. Bennett. 1997. Tyrosine phosphorylation at a site highly conserved in the L1 family of cell adhesion molecules abolishes ankyrin binding and increases lateral mobility of neurofascin. *J. Cell Biol.* 137:703–714.

Gil, O.D., T. Sakurai, A.E. Bradley, M.Y. Fink, M.R. Cassella, J.A. Kuo, and D.P. Felsenfeld. 2003. Ankyrin binding mediates L1CAM interactions with static components of the cytoskeleton and inhibits retrograde movement of L1CAM on the cell surface. *J. Cell Biol.* 162:719–730.

Gordon, G.W., G. Berry, X.H. Liang, B. Levine, and B. Herman. 1998. Quantitative fluorescence resonance energy transfer measurements using fluorescence microscopy. *Biophys. J.* 74:2702–2713.

Hlavin, M.L., and V. Lemmon. 1991. Molecular structure and functional testing of human L1CAM: an interspecies comparison. *Genomics.* 11:416–423.

Hortsch, M. 2000. Structural and functional evolution of the L1 family: are four adhesion molecules better than one? *Mol. Cell. Neurosci.* 15:1–10.

Hortsch, M., D. Homer, J.D. Malhotra, S. Chang, J. Frankel, G. Jefford, and R.R. Dubreuil. 1998a. Structural requirements for outside-in and inside-out signaling by *Drosophila* neuroglian, a member of the L1 family of cell adhesion molecules. *J. Cell Biol.* 142:251–261.

Hortsch, M., K.S. O'Shea, G. Zhao, F. Kim, Y. Vallejo, and R.R. Dubreuil. 1998b. A conserved role for L1 as a transmembrane link between neuronal adhesion and membrane cytoskeleton assembly. *Cell Adhes. Commun.* 5:61–73.

Jay, D.G. 2000. The clutch hypothesis revisited: ascribing the roles of actin-associated proteins in filopodial protrusion in the nerve growth cone. *J. Neurobiol.* 44:114–125.

Jefford, G., and R.R. Dubreuil. 2000. Receptor clustering drives polarized assembly of ankyrin. *J. Biol. Chem.* 275:27726–27732.

Kamiguchi, H., and V. Lemmon. 1997. Neural cell adhesion molecule L1: signaling pathways and growth cone motility. *J. Neurosci. Res.* 49:1–8.

Kamiguchi, H., and V. Lemmon. 1998. A neuronal form of the cell adhesion mol-

ecule L1 contains a tyrosine-based signal required for sorting to the axonal growth cone. *J. Neurosci.* 18:3749–3756.

Kamiguchi, H., and F. Yoshihara. 2001. The role of endocytic L1 trafficking in polarized adhesion and migration of nerve growth cones. *J. Neurosci.* 21: 9194–9203.

Kamiguchi, H., M.L. Hlavin, M. Yamasaki, and V. Lemmon. 1998. Adhesion molecules and inherited diseases of the human nervous system. *Annu. Rev. Neurosci.* 21:97–125.

Kuhn, T.B., M.F. Schmidt, and S.B. Kater. 1995. Laminin and fibronectin guideposts signal sustained but opposite effects to passing growth cones. *Neuron.* 14:275–285.

Lemmon, V., K.L. Farr, and C. Lagenaur. 1989. L1-mediated axon outgrowth occurs via a homophilic binding mechanism. *Neuron.* 2:1597–1603.

Lin, C.H., and P. Forscher. 1995. Growth cone advance is inversely proportional to retrograde F-actin flow. *Neuron.* 14:763–771.

Long, K.E., H. Asou, M.D. Snider, and V. Lemmon. 2001. The role of endocytosis in regulating L1-mediated adhesion. *J. Biol. Chem.* 276:1285–1290.

Mitchison, T.J., and L.P. Cramer. 1996. Actin-based cell motility and cell locomotion. *Cell.* 84:371–379.

Mitchison, T., and M. Kirschner. 1988. Cytoskeletal dynamics and nerve growth. *Neuron.* 1:761–772.

Miyawaki, A., and R.Y. Tsien. 2000. Monitoring protein conformations and interactions by fluorescence resonance energy transfer between mutants of green fluorescent protein. *Methods Enzymol.* 327:472–500.

Mohler, P.J., A.O. Gramolini, and V. Bennett. 2002. The ankyrin-B C-terminal domain determines activity of ankyrin-B/G chimeras in rescue of abnormal inositol 1,4,5-trisphosphate and ryanodine receptor distribution in ankyrin-B (−/−) neonatal cardiomyocytes. *J. Biol. Chem.* 277:10599–10607.

Nagai, T., K. Ibata, E.S. Park, M. Kubota, K. Mikoshiba, and A. Miyawaki. 2002. A variant of yellow fluorescent protein with fast and efficient maturation for cell-biological applications. *Nat. Biotechnol.* 20:87–90.

Nakai, Y., and H. Kamiguchi. 2002. Migration of nerve growth cones requires detergent-resistant membranes in a spatially defined and substrate-dependent manner. *J. Cell Biol.* 159:1097–1108.

Needham, L.K., K. Thelen, and P.F. Maness. 2001. Cytoplasmic domain mutations of the L1 cell adhesion molecule reduce L1-ankyrin interactions. *J. Neurosci.* 21:1490–1500.

Nuckolls, G.H., L.H. Romer, and K. Burridge. 1992. Microinjection of antibodies against talin inhibits the spreading and migration of fibroblasts. *J. Cell Sci.* 102:753–762.

Schaefer, A.W., H. Kamiguchi, E.V. Wong, C.M. Beach, G. Landreth, and V. Lemmon. 1999. Activation of the MAPK signal cascade by the neural cell adhesion molecule L1 requires L1 internalization. *J. Biol. Chem.* 274: 37965–37973.

Schaefer, A.W., N. Kabir, and P. Forscher. 2002a. Filopodia and actin arcs guide the assembly and transport of two populations of microtubules with unique dynamic parameters in neuronal growth cones. *J. Cell Biol.* 158:139–152.

Schaefer, A.W., Y. Kamei, H. Kamiguchi, E.V. Wong, I. Rapoport, T. Kirchhausen, C.M. Beach, G. Landreth, S.K. Lemmon, and V. Lemmon. 2002b. L1 endocytosis is controlled by a phosphorylation-dephosphorylation cycle stimulated by outside-in signaling by L1. *J. Cell Biol.* 157:1223–1232.

Scotland, P., D. Zhou, H. Benveniste, and V. Bennett. 1998. Nervous system defects of ankyrin$_B$ (−/−) mice suggest functional overlap between the cell adhesion molecule L1 and 440-kD ankyrin$_B$ in premyelinated axons. *J. Cell Biol.* 143:1305–1315.

Sheetz, M.P., D.P. Felsenfeld, and C.G. Galbraith. 1998. Cell migration: regulation of force on extracellular-matrix-integrin complexes. *Trends Cell Biol.* 8:51–54.

Silletti, S., F. Mei, D. Sheppard, and A.M. Montgomery. 2000. Plasmin-sensitive dibasic sequences in the third fibronectin-like domain of L1-cell adhesion molecule (CAM) facilitate homomultimerization and concomitant integrin recruitment. *J. Cell Biol.* 149:1485–1502.

Smilenov, L.B., A. Mikhailov, R.J. Pelham, E.E. Marcantonio, and G.G. Gundersen. 1999. Focal adhesion motility revealed in stationary fibroblasts. *Science.* 286:1172–1174.

Smith, C.L. 1994. Cytoskeletal movements and substrate interactions during initiation of neurite outgrowth by sympathetic neurons in vitro. *J. Neurosci.* 14: 384–398.

Suter, D.M., L.D. Errante, V. Belotserkovsky, and P. Forscher. 1998. The Ig superfamily cell adhesion molecule, apCAM, mediates growth cone steering by substrate-cytoskeletal coupling. *J. Cell Biol.* 141:227–240.

Sydor, A.M., A.L. Su, F.S. Wang, A. Xu, and D.G. Jay. 1996. Talin and vinculin play distinct roles in filopodial motility in the neuronal growth cone. *J. Cell Biol.* 134:1197–1207.

Thelen, K., V. Kedar, A.K. Panicker, R.S. Schmid, B.R. Midkiff, and P.F. Maness. 2002. The neural cell adhesion molecule L1 potentiates integrin-dependent cell migration to extracellular matrix proteins. *J. Neurosci.* 22:4918–4931.

Tomaselli, K.J., L.F. Reichardt, and J.L. Bixby. 1986. Distinct molecular interactions mediate neuronal process outgrowth on non-neuronal cell surfaces and extracellular matrices. *J. Cell Biol.* 103:2659–2672.

Van Camp, G., E. Fransen, L. Vits, G. Raes, and P.J. Willems. 1996. A locus-specific mutation database for the neural cell adhesion molecule L1CAM (Xq28). *Hum. Mutat.* 8:391.

Varnum-Finney, B., and L.F. Reichardt. 1994. Vinculin-deficient PC12 cell lines extend unstable lamellipodia and filopodia and have a reduced rate of neurite outgrowth. *J. Cell Biol.* 127:1071–1084.

Wolff, J.M., R. Frank, K. Mujoo, R.C. Spiro, R.A. Reisfeld, and F.G. Rathjen. 1988. A human brain glycoprotein related to the mouse cell adhesion molecule L1. *J. Biol. Chem.* 263:11943–11947.

Yip, P.M., X. Zhao, A.M. Montgomery, and C.H. Siu. 1998. The Arg-Gly-Asp motif in the cell adhesion molecule L1 promotes neurite outgrowth via interaction with the αvβ3 integrin. *Mol. Biol. Cell.* 9:277–290.

Zhang, X., J.Q. Davis, S. Carpenter, and V. Bennett. 1998. Structural requirements for association of neurofascin with ankyrin. *J. Biol. Chem.* 273: 30785–30794.

Zhou, D., S. Lambert, P.L. Malen, S. Carpenter, L.M. Boland, and V. Bennett. 1998. Ankyrin$_G$ is required for clustering of voltage-gated Na channels at axon initial segments and for normal action potential firing. *J. Cell Biol.* 143: 1295–1304.